Peak Wind Load Comparison: Theoretical Estimates and ASCE 7

Henry W. Tieleman, M.ASCE[1]; Mohamed A. K. Elsayed[2]; and Muhammad R. Hajj, M.ASCE[3]

Abstract: A new procedure to derive the distribution of peak pressure and load coefficients from individual sample records is applied to wind tunnel records obtained from a generic flat-roof model tested at the Univ. of Western Ontario (UWO). The initial step of this procedure requires the identification of the appropriate marginal probability of these records. The corresponding distribution of the peaks is then obtained with the use of the standard translation process. Predicted load coefficients over variable tributary areas as determined from UWO records and based on a preset probability of non-exceedence are compared with the provisions of the ASCE 7 standard. Based on the open-terrain observations, the code provisions generally correspond to relatively low levels of nonexceedence of 84% or less. The ASCE 7 suggested method to estimate the peak pressure coefficients for the suburban environment based on those for the open terrain could be successfully applied to the UWO observations. This, however, is generally not true when performing a similar estimation procedure for peak load coefficients from the Clemson experiments.

DOI: 10.1061/(ASCE)0733-9445(2006)132:7(1150)

CE Database subject headings: Wind loads; Coefficients; ASCE publications; Estimation.

Introduction

Since surface pressures are generally stochastic in nature, their inherent variability should always be addressed when considering their statistical quantities such as mean, standard deviation, root mean square (RMS) and extreme values. It is generally accepted in the wind engineering community that the duration of sample records should be equivalent to 1 h in full scale or 1–2 min for wind tunnel simulation experiments to obtain stable estimates of these quantities. Stable estimates of mean and RMS values can generally be obtained from records of relatively short duration. However, pressure and load peaks may vary excessively from one sample record to another. Consequently, the distribution of the peaks must be obtained from observed peaks of a large number of sample records. For field data this is a problem as wind conditions are seldom stationary and usually vary during periods of 1 h or longer. Although flow stationarity can be achieved in wind tunnels, data acquisition for a large number of sample records may become a problem, as excessive wind tunnel time and data analysis would be required. For the safe design and for comparison studies of field and laboratory observations, it behooves the designer to use stable estimates of peak forces at some predetermined level of nonexceedence.

In previous work [Tieleman and Hajj (2004)], we applied a theoretical method to obtain estimates of the distribution of peak wind loads from their individual time histories. The method, initially developed by Sadek and Simiu (2002) at the National Institute of Standards and Technology, yields wind load provisions at different levels of nonexceedence. The previous work involved records of the surface pressure coefficients and load coefficients obtained from wind tunnel experiments on a 1:50 scale model of the Wind Engineering Research Field Laboratory (WERFL) experimental building at Texas Tech Univ. Results of individual point-pressure coefficients and load coefficients, the latter representing the pressure forces on a tributary area of two sets of eight pressure taps, were obtained for seven different flow conditions with the turbulence intensity at roof height varying between 7.1 and 19.3%. For each flow condition and each azimuth angle a total of 16 repeat records were analyzed. The results showed that the time histories of the non-Gaussian pressure and load coefficients observed under separated shear layers on the upper surface (roof) of the WERFL model were best represented with the three-parameter gamma distribution. Once the parameters of this distribution were established for a particular record using the method of moments, the distribution of the peaks was estimated with the use of a standard translation process. With the established parameters for the assumed Type I Extreme Value (Gumbel) distribution, peak values at any level of nonexceedence could be obtained. The results revealed that the peak distributions obtained from different repeat records were not identical. Their observed variability with respect to the peak distribution obtained with the method of moments based on the observed peaks of the 16 individual records fell in a range of ±10% for the loads.

The objective of this work is to compare predicted load coefficients over variable tributary areas as determined from UWO records, and based on a preset probability of nonexceedence, with the provisions of the ASCE 7 standard. The distribution of peak

[1]Professor Emeritus, Dept. of Engineering Science and Mechanics, Virginia Polytechnic Institute and State Univ., Blacksburg, VA 24061-0219. E-mail: tieleman@vt.edu

[2]Graduate Assistant, Dept. of Engineering Science and Mechanics, Virginia Polytechnic Institute and State Univ., Blacksburg, VA 24061-0219. E-mail: melsayed@vt.edu

[3]Professor, Dept. of Engineering Science and Mechanics, Virginia Polytechnic Institute and State Univ., Blacksburg, VA 24061-0219 (corresponding author). E-mail: mhajj@vt.edu

Note. Associate Editor: Kurtis R. Gurley. Discussion open until December 1, 2006. Separate discussions must be submitted for individual papers. To extend the closing date by one month, a written request must be filed with the ASCE Managing Editor. The manuscript for this paper was submitted for review and possible publication on May 31, 2005; approved on November 14, 2005. This paper is part of the ***Journal of Structural Engineering***, Vol. 132, No. 7, July 1, 2006. ©ASCE, ISSN 0733-9445/2006/7-1150–1157/$25.00.

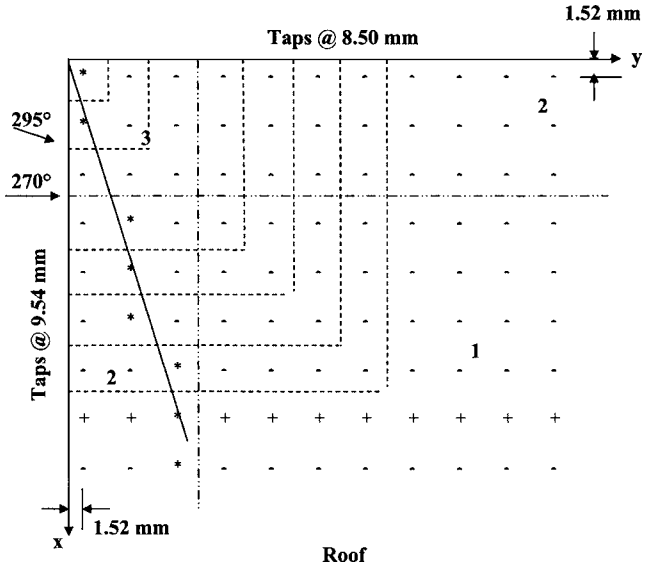

Fig. 1. Layout of roof pressure taps near roof corner with tributary zones

pressure and load coefficients from individual sample records are derived from the application of the Sadek–Simiu peak analysis procedure to time histories of pressure and load coefficients from a generic model study conducted in the Boundary Layer Wind Tunnel Laboratory at the Univ. of Western Ontario (UWO) (Ho et al. 2005). Additional comparisons of peak load coefficients from experiments conducted at Clemson Univ. with the ASCE provisions are also presented.

Experiments

The UWO experiments were conducted in two different turbulent flows representing open and suburban terrain; with roof-height turbulence intensities of 18.2 and 24.6%, respectively. For the open-terrain exposure at scales of 1:100 and 1:50 the corresponding roughness lengths are estimated at 50 and 25 m, representing terrain with low mature crops and long grass respectively (Tieleman 2003a). For the suburban exposure with an average building height of 10 m, the blending height of 25 m is considered appropriate. With the observed turbulence intensity at this height of 25%, the full-scale roughness length would be 0.54 m, which is representative of a suburban terrain exposure (Grimmond et al. 1998).

Pressure measurements were conducted on a nearly flat-roof model (roof slope 1/4:12) that has the dimensions of 244 mm × 381 mm × 98 mm. The pressure records were obtained at 500 samples/s for the duration of 100 s. The nearly square mesh of the pressure tap layout on the roof of the UWO model consists of 300 taps. Time histories for two azimuth angles of 270 and 295° were analyzed. The data analysis, performed in this work, is concerned with the pressure records near the roof corner, where the pressure taps are located in a denser pattern (Fig. 1). In the direction of the long side of the building, parallel to the roof ridge (x direction), the distance between the taps is 9.54 mm, while in the y direction the distance between the taps is 8.50 mm. In both directions the first row of taps is located 1.52 mm from the leading edge. Because of the dense mesh of pressure taps at the roof corner, the UWO model experiment provides a unique opportunity to obtain peak load estimates for varying tributary areas where the pressures changes appreciably over short distances, and to compare the results with the provisions from the ASCE 7-02 standard (ASCE 2002). Four roof tap categories exist, each representing a different area over which the instantaneous pressure is considered uniform: the corner tap area is 36.31 mm^2, the taps along the x and y axes represent areas of 55.05 and 53.50 mm^2, respectively, and the interior taps 81.13 mm^2. Similar results are obtained for varying areas on the walls of the model where the tap density is much less, but where the pressure distribution is considered to be more uniform.

Peak Distribution Analysis

A short review of the procedure used to determine the probability of nonexceedence is presented here. The first step in the analysis is to establish the distribution of the parent time history, for which the gamma distribution, given by

$$f(x) = [(x-\mu)/\beta]^{\gamma-1} \exp\{[-(x-\mu)/\beta]\}/[\beta\Gamma(\gamma)] \quad \text{for } x > \mu \tag{1}$$

is the most likely candidate. In Eq. (1), γ, β, and μ are referred to as shape, scale, and location parameters. They can be determined from the skewness S, and mean X, and RMS x', values according to the following relations:

shape parameter

$$\gamma = (2/S)^2 \tag{2}$$

scale parameter

$$\beta = x'S/2 \tag{3}$$

location parameter

$$\mu = X - (2x'/S) \tag{4}$$

For low skewness values ($S < 0.35$), the shape parameter takes on large values and the gamma function $\Gamma(\gamma)$ approaches infinity. Under these conditions, the normal distribution is the more appropriate distribution. The condition that $x > \mu$ in Eq. (1) requires that records consisting of negative suction pressures, such as those observed in separation regions, be multiplied by -1. For time histories obtained in stagnation regions for which the tail of the peak distribution is positive, this condition is automatically satisfied.

The second step in the analysis is to obtain the cumulative distribution function (CDF) with the prescribed mapping procedure as outlined in ASCE (2002) and Grimmond et al. (1998). From the obtained CDF, one derives by differentiation, the probability density function (PDF) of the peaks from which the mean (P) and the RMS (p') follows. Assuming that the Extreme Value Distribution Type 1 (Gumbel) is appropriate, its two parameters can be obtained with the method of moments

$$\beta = (p'\sqrt{6})/\pi$$

and

$$\mu = P - 0.5772\beta \tag{5}$$

Hence, with the CDF for the Gumbel distribution

$$F(p) = \exp\{-\exp[-(p-\mu)/\beta]\} \quad (6)$$

an estimated peak value for any level of nonexceedence can be obtained. On a double logarithmic (Gumbel) paper, the Gumbel distribution plots as a straight line

$$-\{\ln[-\ln F(p)]\} = p/\beta - \mu/\beta \quad (7)$$

with slope $1/\beta$. For a set of peaks with a great deal of scatter its standard deviation and therefore β have large magnitudes leading to smaller slopes of the Gumbel plot of these peaks. It should be noted here that, in cases where a set of peaks is available, the Gumbel parameters, β and μ, can be directly evaluated from the moment estimators Eq. (5).

Results

The analysis of the UWO records was carried out for two azimuth angles of 270 and 295°, and for two incident flows with 18.2 and 24.6% roof-height turbulence intensities representing open and suburban terrain, respectively. The pressure and force coefficients presented in the ASCE code are based on 3 s gust speeds. For comparison with wind tunnel results that are generally based on an hourly mean wind speed, the code provisions must be converted by multiplying the listed pressure and load coefficients by the square of the velocity ratio $V_3/V_{3,600}$ or 2.33. In the commentary of the ASCE code the argument is made that the GC_p values for open terrain with scattered obstructions may also be used to estimate the coefficients for suburban exposures provided the correct dynamic pressure (velocity pressure) for this exposure category is used. In order to check the validity of this simplification, the pressure coefficients obtained for the open terrain exposure were multiplied by the square of the roof height velocity ratio $(V_H)_{\text{open}}$ and $(V_H)_{\text{suburban}}$ or 1.56 to compare with the observed suburban coefficients. In the discussion of the results that follows, the "predicted" coefficients are derived with the Sadek–Simiu technique, while the "estimated" coefficients refer to the coefficients for higher turbulence flows (suburban) derived from those for lower turbulence intensity (open terrain).

Because of the dense mesh of pressure taps on the roof corner, the UWO model experiment provides a unique opportunity to obtain peak-load estimates for various tributary areas. Fig. 6-11B of ASCE 7-02 recognizes three zones on gable roofs. The first is a corner area that is referred to as Zone 3. It is a square area with side "a" that corresponds to one tenth of the model width. For the UWO model "a" is equal to 24.4 mm. In the analysis presented here, we have adapted the distance "a" that is slightly larger to form an area that includes the nine corner taps (Fig. 1). Zone 2, located along the roof edges, has a width of the same distance a and extends from the border of Zone 3 at one corner to that of the adjacent corner. The remainder (interior) of the roof is designated as Zone 1.

The pressure tap layout at the roof corner together with the three zones as recognized by ASCE 7 is presented in Fig. 1. This figure also displays the tributary areas emanating from the roof corner for which the wind loads were obtained. The + symbols represents the taps that are located along a line perpendicular to the roof edge (x axis) at $x/H=0.7$. These taps are designated as Set I. The taps marked with the $*$ symbol (Set II) are located approximately along a straight line from the roof corner and make an angle of 15° with respect to the same roof edge. Here, s is the distance along the ray measured from the roof corner (Fig. 1).

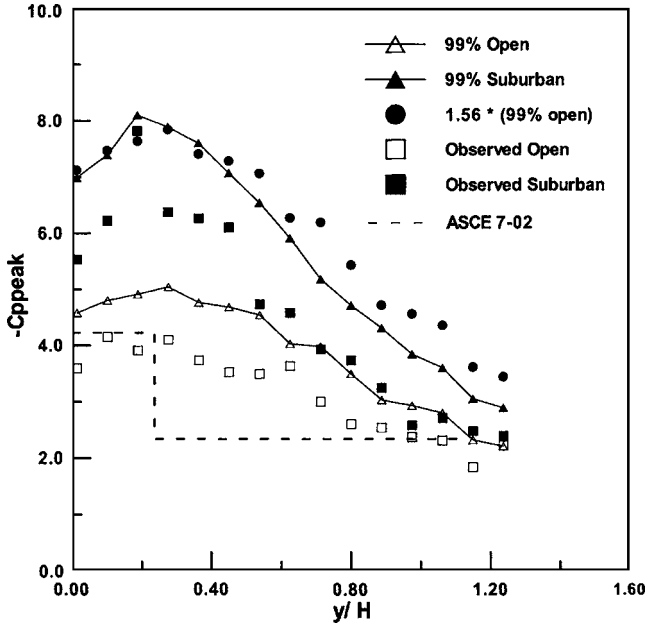

Fig. 2. Peak pressure coefficients distribution for Set I

Fig. 2 displays the peak pressure coefficients from Set I for the azimuth angle of 270 degrees (flow parallel to the line of pressure taps). In addition to the observed peak pressure coefficients, the predicted peak pressure coefficients at a level of 99% nonexceedence for both flow regimes are also presented. Both observed and predicted peak pressure coefficients for the suburban exposure exceed those of the open-terrain exposure by about 50%. The estimation of the former based on the latter by multiplying the open terrain peak pressure coefficients by the square of the roof-height velocity ratio (1.56) is acceptable. Moreover, the ASCE code provisions of $GC_p=-4.2$ for Zone 2 and $GC_p=-2.3$ for Zone 1 do not match the peak pressure coefficients at the 99% nonexceedence level for the open terrain configuration very well in the part of Zone 1 that is adjacent to Zone 2. By referring to Fig. 1, one observes that the three data points closest to the leading edge correspond to Zone 2, while the remainder of the data points of Set I are located in Zone 1. Of course, at the intersection of Zones 2 and 1 the pressure coefficients do not undergo a sudden change but instead must vary gradually.

Similar results are presented for the peak pressure coefficients of Set II (Fig. 3). The variability of the results must be attributed to the fact that the selected pressure taps deviate from the straight line (Fig. 1) as a result of being part of the square mesh of taps. The two data points closest to the roof corner of Fig. 3 correspond to pressure taps located in Zone 3, with the remainder of the data points of Set II belonging to Zone 2. The estimation of the peak pressure coefficients for the suburban exposure from the ones observed from the open-terrain exposure is again excellent. The first two taps of this group fall in the corner Zone 3 for which $GC_p=-6.51$ while the corresponding observed peak pressure coefficients fall between −8 and −10 and the corresponding Sadek–Simiu predictions are approximately −12. The remaining six taps are located in Zone 2 for which the ASCE code prescribes $GC_p=-4.2$ that is an adequate prediction for the observations at $s/H>0.6$ but falls well below the Sadek–Simiu estimates of −7.

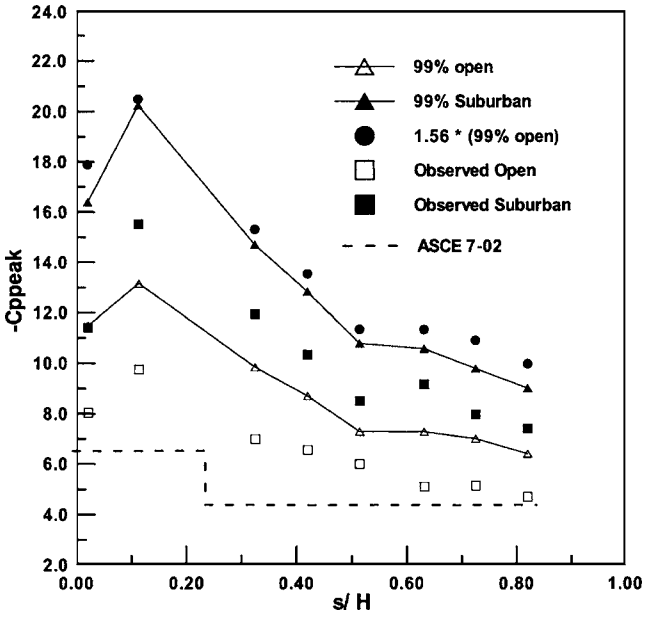

Fig. 3. Peak pressure coefficients distribution for Set II

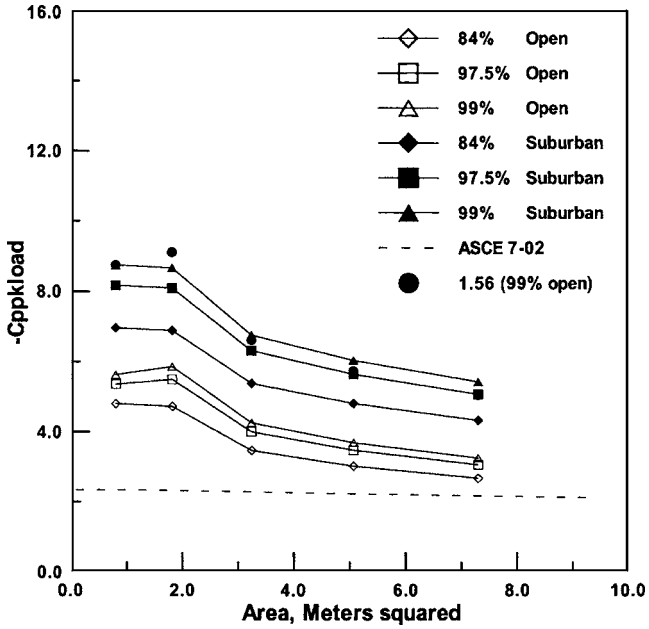

Fig. 5. Peak load coefficients for tributary areas of Fig. 5

The code provisions fall well below the predicted open-terrain peak pressure coefficients at the 99% nonexceedence level. Again, the prediction of the peak pressure coefficients for the suburban terrain based on those for the open terrain is quite satisfactory.

Next, we analyze the peak roof loads in the form of peak load coefficients for Zones 1, 2, and 3 or a combination of these zones, and also for wall Regions 4 and 5. To obtain the time histories of the loads coefficients, the individual time histories of the pressure coefficients are multiplied by a weighting coefficient based on its representative area as a fraction of the total area under consideration. The load coefficients are then obtained by adding the weighted time histories. The peak load coefficients for the respective areas in full scale (1:50) for the open and suburban terrain exposures are shown as open and closed symbols, respectively, for the different fractiles. The figures also display the corresponding provisions from ASCE 7-02 and the estimated peak load coefficients for the suburban exposure based on those of the open terrain exposure for the 99% fractile. All load coefficients shown in these figures are based on an hourly mean wind speed.

Fig. 4 shows the peak load coefficients on the square areas emanating from the roof corner consisting of 1, 4, 9, 16, 25, and 36 taps, respectively, and for an azimuth angle of 295° (Fig. 1). The data for the smallest three areas correspond to Zone 3, while the larger areas are a combination of all three zones. Except for the load coefficients on the corner area, the code provisions match the predicted open-terrain results quite well. Fig. 5 shows the

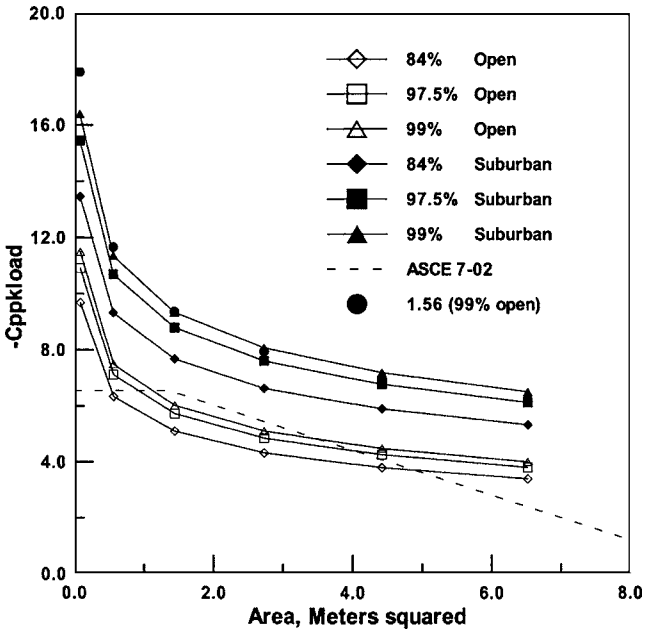

Fig. 4. Peak load coefficients for tributary areas of Fig. 1

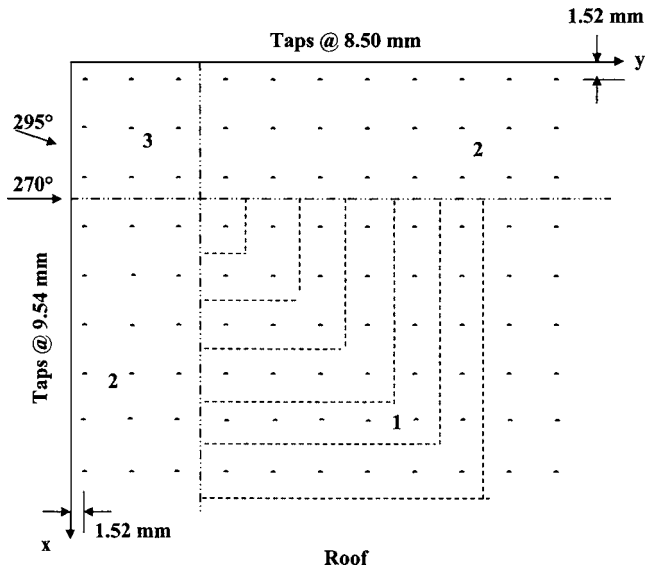

Fig. 6. Tributary areas for Zone 1

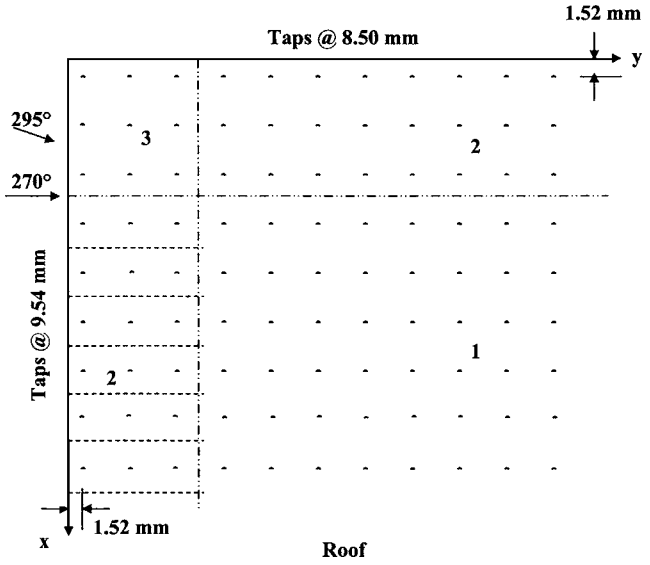

Fig. 7. Tributary areas for Zone 2

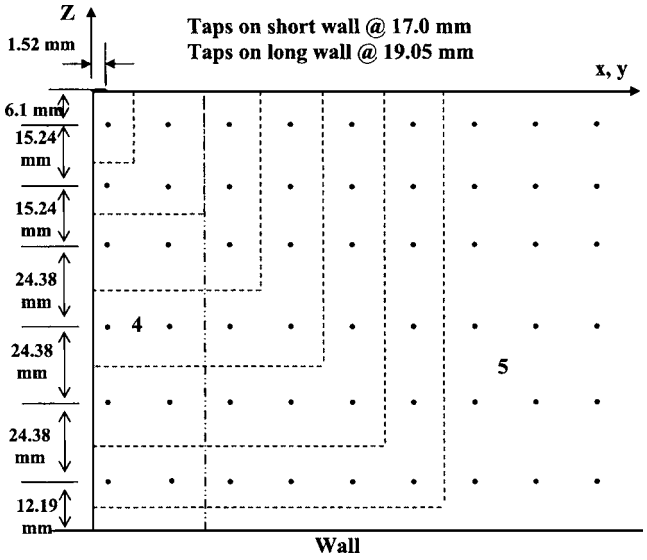

Fig. 9. Tributary wall areas of Regions 4 and 5

peak load coefficients over square areas that are entirely located in Zone 1, but now emanating from the pressure tap just outside Zone 3 (Fig. 6). The peak load coefficients (azimuth 295°) for the 84, 97.5, and 99% fractiles exceed the ASCE 7-02 provisions. On the other hand, the load coefficients for the suburban exposure estimated on the basis of the open terrain exposure is actually quite good. Tributary areas for Zone 2 are presented in Fig. 7. The peak load coefficients in Zone 2, displayed for an azimuth of 295°, are presented in Fig. 8. These coefficients, presented for the smallest area, are based on the three taps in Zone 2 bordering Zone 3 (Fig. 7). Increases in the area are achieved by including the next three taps in succession. The results are very similar to those presented in Figs. 4 and 6 except for the open terrain exposure the code provisions fall well below the estimated peak loads coefficients derived with the Sadek–Simiu analysis.

Tributary wall areas for Regions 4 and 5 are presented in Fig. 9. The peak load coefficients on the wall of the short side of the model in the separation zone (azimuth 270°) are presented in Fig. 10. The first and second points on this figure (area less than 2.5 m^2) represent the load coefficients for the area encompassed by the first and the four taps in the upper corner adjacent to the leading wall edge (Region 4). The next points on Fig. 10 (areas larger than 2.5 m^2) represent areas that are located in both Regions 4 and 5 (Fig. 9). The code provisions for the load coefficients of the wall regions in separated flow fall slightly below the predicted open-terrain results at the 84% level of nonexceedence.

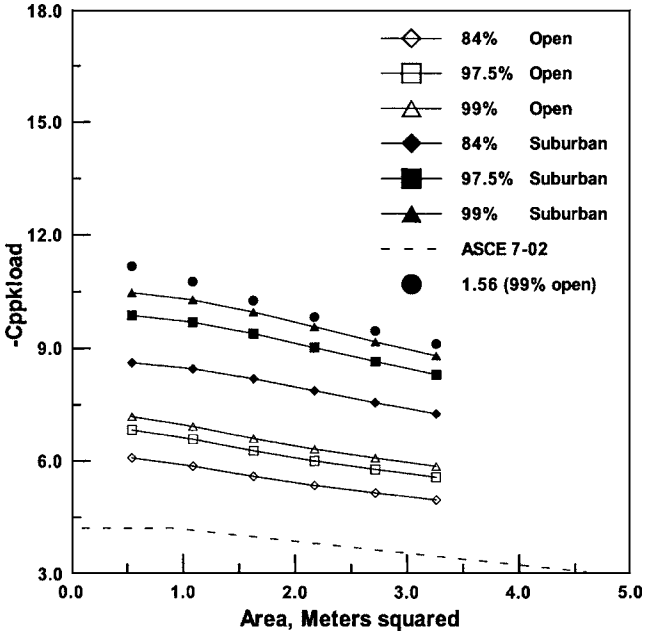

Fig. 8. Peak load coefficients for tributary areas of Fig. 7

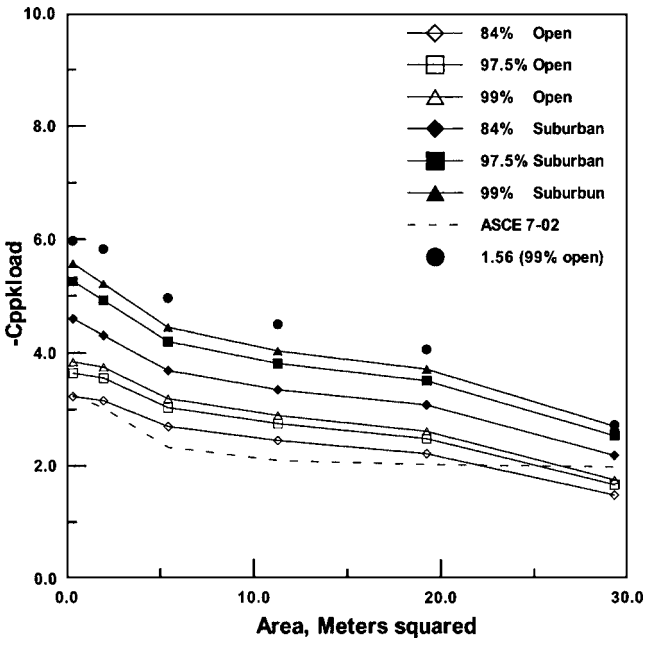

Fig. 10. Peak load coefficients for tributary areas of Fig. 9 with azimuth 270° (zone of flow separation)

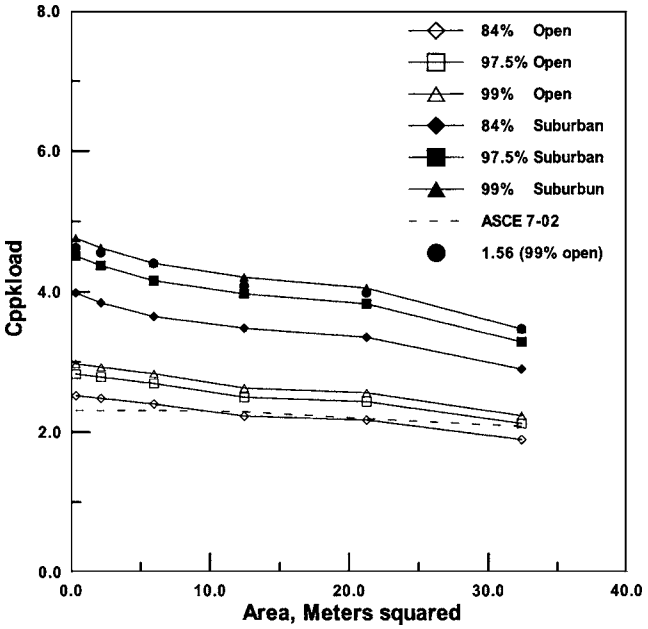

Fig. 11. Peak load coefficients for tributary areas of Fig. 9 with azimuth 295° (zone of positive mean pressure)

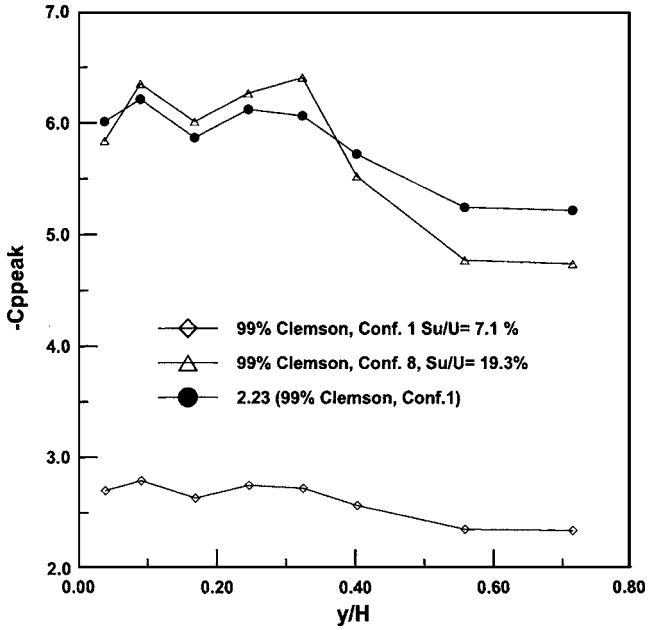

Fig. 13. Peak pressure coefficients for pressure tap Set A

While, the peak load coefficients for the suburban case based on the data for the open terrain exposure exceed the 99% level of nonexceedence predicted from the UWO observations for the suburban-terrain exposure.

The pressures and loads on the upwind wall are generally positive and skewed in the positive direction. The results presented in Fig. 11 for an azimuth angle of 295° start with an area associated with the single tap near the roof corner and increases by incorporating the results of additional taps (Fig. 9). The skewness of the pressure from this tap is rather low, but increases for the larger areas. Again the estimation of the peak loads for the suburban exposure based on those of the open-terrain exposure is quite satisfactory. The ASCE 7-02 provisions match the 84% fractile peak load coefficients from the open terrain exposure, while for higher levels of nonexceedence, the Sadek–Simiu derived load coefficients exceed those of the code.

In Fig. 12, the peak load coefficients for the pressure tap Set I are compared with similar results of pressure tap Set A from the Clemson experiment. The numbers listed in the figure represent the different floor roughness configurations that are discussed in detail in Tieleman et al. (2003). The roof-height turbulence intensities of the Clemson data vary between 7.1 and 19.3%. The results undoubtedly reveal that the magnitude of the coefficients for the different configurations increase appreciably with the incident

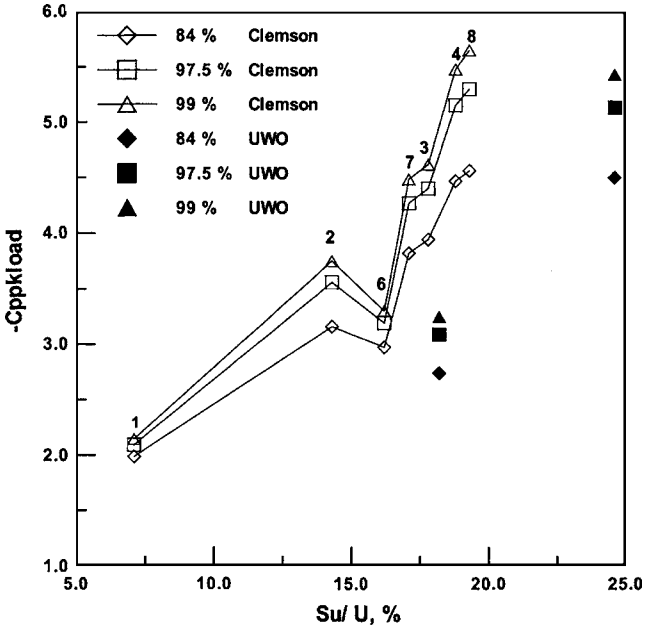

Fig. 12. Peak load coefficients for pressure tap Sets A and I

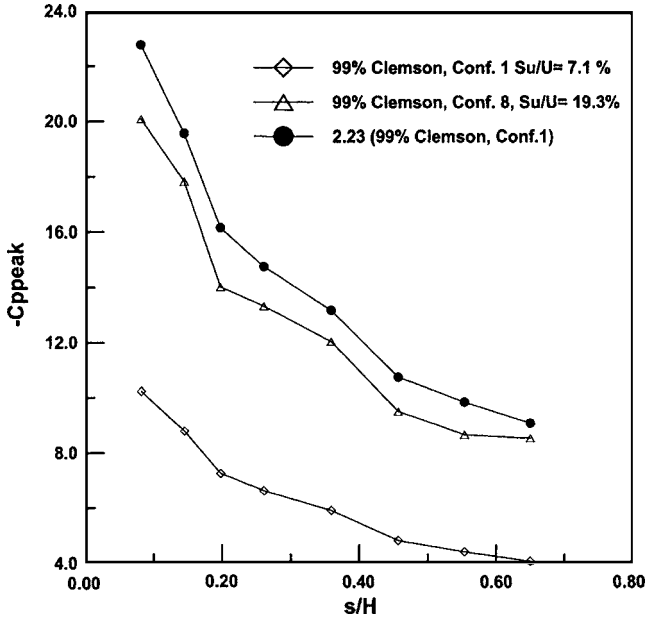

Fig. 14. Peak pressure coefficients of pressure tap Set B

Table 1. Estimated Peak Load Coefficients

Pressure tap set	Cpp 99%	Exposure number	Cpp 99%	Exposure number	Square of velocity ratio	Estimated Cpp, 99%	Exposure number	Source
A	2.07	1	3.49	6	1.56	3.23	6	Clemson
A	2.07	1	4.12	7	2.47	5.59	7	Clemson
A	2.07	1	4.54	3	1.63	3.37	3	Clemson
A	2.07	1	5.14	4	1.90	3.93	4	Clemson
A	2.07	1	5.07	8	2.23	4.46	8	Clemson
I	3.25	Open terrain	5.43	Suburban	1.56	5.07	Suburban	U.W.O
B	7.24	1	10.7	6	1.56	11.29	6	Clemson
B	7.24	1	11.48	7	2.47	17.88	7	Clemson
B	7.24	1	14.35	3	1.63	11.80	3	Clemson
B	7.24	1	15.99	4	1.90	13.76	4	Clemson
B	7.24	1	15.67	8	2.23	16.15	8	Clemson

turbulence intensity for open-terrain exposures with turbulence intensities exceeding 10% at a height of 4 m (Tieleman 2003b). Consequently, the provisions of ASCE 7 listing just a single pressure or load coefficients for the open-terrain category (C) must be investigated. The discontinuity of the peak load coefficients in Fig. 12 for exposure #6 is attributed to the low level of the small-scale turbulence of the incident flow (Tieleman et al. 2003).

The presentation of the UWO peak pressure and load coefficients have revealed that those coefficients for the suburban terrain can be estimated reasonably well from the corresponding open-terrain results. Expressed in more general terms, the coefficients obtained in a flow with larger roof-height turbulence intensity (UWO: 24.6%) can be estimated from observations obtained in a flow with lower turbulence intensity (UWO: 18.2%). This requires that the latter coefficients be adjusted and are based on the roof-height dynamic pressure associated with the higher turbulence flow. This can be achieved by multiplying the peak coefficients for the low-turbulence flow with the square of the ratio of the roof-height velocity for the low turbulence flow with that for the high-turbulence flow. This approach is now tested for the Clemson wind tunnel observations of the two pressure tap Sets A and B (Tieleman et al. 2003) that correspond closely to Sets I and II of the UWO experiments. The best results were obtained from the estimation of the peak pressure coefficients for configuration #8, based on those from configuration No. 1 (Figs. 13 and 14). For this case, the multiplication factor for the peak pressure coefficients of exposure #1 is 2.23 (Table 1). The estimates for Set A are quite adequate while the estimation for the Set B data exceeds the observations. A similar estimation procedure applied to the peak pressure coefficients for the configurations Nos. 4 and 6 for both Sets A and B turned out to be less successful. Estimates of peak load coefficients for the Clemson Sets A and B and the UWO Set I, are presented in Table 1. The estimation of the load coefficients associated with higher turbulence intensities are based on those of the lower turbulence intensities of exposure No. 1 and the UWO open terrain exposure. Comparison of the estimated peak load coefficients (column 7 of Table 1) with the predictions obtained with the Sadek–Simiu method reveals (column 4 of Table 1) that the ASCE 7 proposed method for the estimation of peak load coefficients leads to unreliable results.

Conclusions

A new procedure to derive the distribution of peak pressure and load coefficients from individual sample records is applied to wind tunnel records obtained from a generic flat-roof model tested at the UWO. Different cases of peak pressure and peak load coefficients on the roof and walls of the model in two different turbulent flows are analyzed. These flows represent an open-terrain and suburban exposure, respectively. By analyzing the pressure records to obtain peak values at 99% nonexceedence, we were able to make the .

For the case where the flow is normal to the leading roof edge, the Sadek–Simiu derived peak pressure coefficients along a line normal to the leading edge (Set I) exceed the observed coefficients. The ASCE prescribed coefficients in Zone 2 match the open terrain peak pressure coefficients at a 99% nonexceedence level. On the other hand, the ASCE 7 prescribed peak coefficients in Zone 1 match open terrain peak pressure coefficients at a 99% nonexceedence level only for taps further away from Zone 2. For the taps located along a line making 15° with the leading edge (x axis), the Sadek–Simiu derived peak pressure coefficients for the open-terrain exposure exceed the building code provisions.

For all cases investigated, the suburban peak and load coefficients exceed invariably those obtained from the open-terrain exposure experiments. The results from both Clemson and UWO experiments show that the peak load coefficients vary appreciably with the incident turbulence intensity. For the UWO experiments, the estimation process of the peak pressure and load coefficients for the suburban terrain based on those for the open-terrain exposure works reasonably well. However, the same estimation technique applied to the peak load coefficients from the experiments conducted in the Clemson wind tunnel provides generally unreliable results. As such, using dynamic pressures to convert wind load data from one exposure to another may be premature since it appears to work well on one data set but not the other. The code provisions for the peak load coefficients match or fall below those predicted with the Sadek–Simiu analysis for a nonexceedence level of 84%.

Acknowledgments

The writers gratefully acknowledge Dr. T. C. E. Ho of the Boundary Layer Wind Tunnel Laboratory at the University of Western Ontario for making the data records available. The ongoing support from Dr. Sadek and Dr. Simiu for the data analysis is greatly appreciated.

Notation

The following symbols are used in this paper:

C_p = pressure coefficient;
C_{pp} = peak pressure coefficient;
C_{ppkload} = peak load coefficient;
$F(p)$ = probability density function of variable p;
$f(x)$ = gamma distribution of variable x;
G = gust effect factor;
H = model height;
P = mean pressure;
p = pressure;
p' = standard deviation of p;
S = skewness;
S_u = standard deviation of velocity fluctuations;
s = coordinate of Set II pressure taps (Fig. 1);
U = mean velocity;
x = variable, also x roof coordinate;
x' = standard deviation of variable x;
y = y roof coordinate;
z = vertical coordinate;
β = scale parameter;
$\Gamma(.)$ = gamma function;
γ = shape parameter; and
μ = location parameter.

References

ASCE. (2002). "Minimum design loads for buildings and structures." *ASCE 7-02*, Reston, Va.

Grimmond, C. S. B., King, T. S., Roth, M., and Oke, T. R. (1998). "Aerodynamic roughness of urban areas derived from wind observations." *Boundary-Layer Meteorol.*, 89, 1–24.

Ho, T. C. E., Surry, D., Morrish, D., and Kopp, G. A. (2005). "The UWO contribution to the NIST aerodynamic database for wind loads on low buildings: Part I. Archiving format and basic aerodynamic data." *J. Wind. Eng. Ind. Aerodyn.*, 93, 1–30.

Sadek, F., and Simiu, E. (2002). "Peak non-Gaussian wind effects for database-assisted low-rise building design." *J. Eng. Mech.*, 128(5), 530–539.

Tieleman, H. W. (2003a). "Roughness estimation for wind-load simulation." *J. Wind. Eng. Ind. Aerodyn.*, 91, 1163–1173.

Tieleman, H. W. (2003b). "Wind tunnel simulation of wind loading on low-rise structures: A review." *J. Wind. Eng. Ind. Aerodyn.*, 91, 1627–1649.

Tieleman, H. W., and Hajj, M. R. (2004). "Theoretically estimated peak wind loads." *Proc., 5th Int. Colloquium on Bluff Body Aerodynamics and Applications*, Ottawa. July 11–15, 2004, 359–362.

Tieleman, H. W., Ge, Z., Hajj, M. R., and Reinhold, T. A. (2003). "Pressures on a surface-mounted rectangular prism under varying incident turbulence." *J. Wind. Eng. Ind. Aerodyn.*, 91, 1095–1115.